Extended Object Tracking with Exploitation of Range Rate Measurements

STEVEN BORDONARO
PETER WILLETT
YAAKOV BAR-SHALOM
MARCUS BAUM
TOD LUGINBUHL

In active sonar and radar target tracking, measurements consist of position and often also include range rate. Tracking algorithms use these measurements over time to estimate target state comprising position, velocity and, where applicable, turn rate. In most cases there is an underlying assumption in the tracking algorithm that the target is a "point target" (i.e. the target has no physical extent). Another common assumption is that at most one measurement per scan originates from the target. For certain combinations of transmitted waveform and target type, the resolution of the waveform is such that the target is "over-resolved" (i.e. the sensor resolution is high enough that closely spaced scatter centers can be resolved). For such cases the point target assumption must be replaced with an extended target assumption. This work provides a methodology to exploit the extended nature of the target for the case of a rigid target whose spatial characteristics are fixed with respect to the line of motion. By employing a combination of the expectation maximization (EM) algorithm and allowing more than one measurement per scan to originate from the target, a technique is developed that uses a single scan of raw measurements that include range, bearing and range rate to provide an estimate of target position, velocity, heading and turn rate. This single scan estimate is then used in a nearly constant turn rate extended Kalman filter to provide a multi-scan estimate of the target state.

Manuscript received December 30, 2015; revised May 11, 2016; released for publication January 16, 2017.

Refereeing of this contribution was handled by Paolo Braca.

Authors' addresses: S. Bordonaro and T. Luginbuhl, Naval Undersea Warfare Center, Newport, RI 02841 (E-mail: steven.bordonaro@navy.mil, tod.luginbuhl@navy.mil). P. Willett, Y. Bar-Shalom, and M. Baum, Dept. of Electrical and Computer Engr., University of Connecticut, Storrs, CT 06269-2157, USA (E-mail: willett@engr.uconn.edu, ybs@engr.uconn.edu, baum@engineer.uconn.edu).

I. INTRODUCTION

In active sonar and radar target tracking systems, the goal is often to provide an estimate of the target's state using measurements of range, bearing and range rate. Target dynamics are best modeled in Cartesian coordinates and consist of position, velocity and often include acceleration or turn rate. Common models for target dynamics are the nearly constant velocity, nearly constant acceleration and coordinated turn models [1].

In the formulation of the tracking algorithm it is common to assume that the target has no physical extent. This assumption is reasonable if the resolution of the transmitted waveform is greater than or equal to the size of the target. If, however, the resolution of the measurements is small enough that the spatial characteristics of the target can be measured, this "point target" assumption must be relaxed.

If the sensor is capable of resolving individual measurement sources within an extended target and detailed knowledge is available to model these sources, the target can be modeled as a set of discrete measurements sources within an extended object [2]. An alternative is to estimate the overall shape of the target as opposed to individual components. Within this shape estimation approach, numerous models exist. Two approaches that represent the extended target as an ellipse are [14], which uses symmetric, positively definite (SPD) random matrices; and the approach of [3] which employs a random hypersurface model (RHM). The RHM approach has been extended to more complex shapes in [2] by using star-convex RHMs. Irregular shapes are handled in [15] by using multiple (possibly overlapping) ellipses. Another approach to modeling spatial extent uses the assumption that the number of target measurements is Poisson distributed, with the measurement(s) drawn from a spatial distribution [9], [10], [11].

While these approaches are excellent and fairly liberal with regards to shape, a different approach is chosen here that aims to fully exploit the range rate measurements at the expense of using a somewhat more restrictive target model. The target model chosen in this research is that of a target "template" that characterizes the locations of target highlights (i.e. the active reflectors of the target). While the size and orientation of the target is unknown, the relationships of the highlight locations are assumed to be known a priori. It is also assumed that the target is rigid and has spatial characteristics that are fixed with respect to the line of motion. (The model can be viewed as a parameterized version of a "discrete" spatial distribution, as discussed in [5], [10]. The idea of using a set of reflectors can also be found in [13]; however, in [13] the relative positions of the reflectors are based on a known target size, while in the model proposed here, the size is unknown.) With this parametrized model, a single scan estimate of position, velocity, heading and turn rate can be made. This single scan estimate can then be utilized in a multi-scan tracker

(e.g. an extended Kalman filter) with a coordinated turn motion model (nearly constant turn rate) [1].

To provide the target estimate, the measurements from the extended target must be assigned to the individual target highlights. This is achieved by employing a combination of the EM algorithm and a version of the probabilistic multi-hypothesis tracker (PMHT) association model [18]. Unlike many tracking approaches, the PMHT (even for a single point target) does not assume there is at most a single measurement per target. There is therefore a natural compatibility between the PMHT and extended objects, which have multiple measurements per target. Also advantageous is that the algorithm is very flexible and easy to extend [22]. A pertinent example of this is that the PMHT has been successfully employed in extended object tracking using random matrices [20], [21]. The relationship of the PMHT association model with spatial distributions is also discussed in [10] and [9].

The combination of this target extent model and EM based estimation results in an algorithm with similar characteristics to one from a different field (image processing). This concept of aligning measured points to a template can be viewed as a version of surface registration. The iterative closest point algorithm (ICP) [23] is a common approach for surface registration. Its extension, the multi-scale EM-ICP [12], uses a similar formulation to the one proposed here; however, the approach of the present paper allows for the more general measurement error model needed for radar/sonar processing and utilizes range rate measurements. The novel aspect of the approach proposed here is the employment of a template based target model and utilization of existing techniques (EM, observed information matrix and the EKF) in an innovative way to exploit the extended nature of the target to improve state estimates.

The remainder of this paper is organized as follows: Section II introduces the model for the extended target and the measurements; Section III describes the approach for single and multi-scan estimation; Section IV provides a simulation of the algorithm and examines the resulting performance and Section V provides some concluding remarks. This paper is a continuation of the work presented in [7], with portions of [7] repeated here for continuity. This paper extends [7] by (i) modifying the measurement model to improve performance, (ii) providing an estimate of the converted measurement error covariance using the observed information matrix and (iii) utilizing the converted measurement in an extended Kalman filter.

II. THE MODEL

A. Extended Target Model with Discrete Reflectors

In active radar and sonar processing, the transmitted signal is reflected off the target and returns to the receiver, resulting in measurements of range, bearing and range rate. The reflections are due to a finite number of strong reflectors, such as the nose and engines of an aircraft or the bow and sail of a submarine. For waveforms with high spatial resolution, it is possible to resolve the individual reflectors from the target as opposed to the integration of all the reflectors. In many cases there is general knowledge of the relative locations of the primary reflectors for a given target class (e.g. a military aircraft), that can reasonably represent a number of targets in that class. Using this premise, an extended target model approach can be developed as in [7].

The target is therefore represented as a set of M highlights (i.e. reflectors) forming a template for a general target. Each reflector, $j = 1 \cdots M$, is specified with a probability of detection, ζ_j, and a position in 2D Cartesian coordinates,

$$\mathbf{t}_j = \begin{bmatrix} x_t(j) \\ y_t(j) \end{bmatrix} \tag{1}$$

relative to the center of the target. While the shape of the target is known, the orientation, ψ, location (of the center), $\mathbf{x} = [x \;\; y]^{\mathrm{T}}$, and size, s, are unknown.

An assumption is made that the direction of travel of the object is along the orientation, ψ, of the target (i.e. the plane flies forward, not sideways).[1] Furthermore, we assume the target is following a coordinated turn (nearly constant speed and turn rate) motion model. Using these assumptions the turn rate, $\dot{\psi}$, and speed, v, can be estimated using a single scan of data.

B. Measurement Model

The measurement vector for a single scan of N measurements for time step k is

$$\mathbf{z}_{\mathrm{RAW}_i}(k) = \begin{bmatrix} r_m(i,k) \\ \alpha_m(i,k) \\ \dot{r}_m(i,k) \end{bmatrix} \qquad i = 1, \ldots, N \tag{2}$$

where the measurement vector includes range, r, bearing, α, and range rate, $\dot{r}$.

The measurement error for the raw measurements is assumed to be Gaussian with covariance matrix

$$R_{\mathrm{RAW}} = \begin{bmatrix} \sigma_r^2 & 0 & \rho\sigma_r\sigma_{\dot{r}} \\ 0 & \sigma_\alpha^2 & 0 \\ \rho\sigma_r\sigma_{\dot{r}} & 0 & \sigma_{\dot{r}}^2 \end{bmatrix} \tag{3}$$

where σ_r, σ_α, and $\sigma_{\dot{r}}$ are the standard deviations of the range, bearing and range rate measurement noise. The correlation coefficient between the range and range rate measurement noise is ρ.

III. ESTIMATION APPROACH

An overview of the new approach is shown in Fig. 1. First the raw measurements from a single scan are

[1]Note that, due to wind forces, the direction of movement of the aircraft, or track, is not necessarily same as the heading. Although this difference is neglected here, the difference may not negligible in certain scenarios.

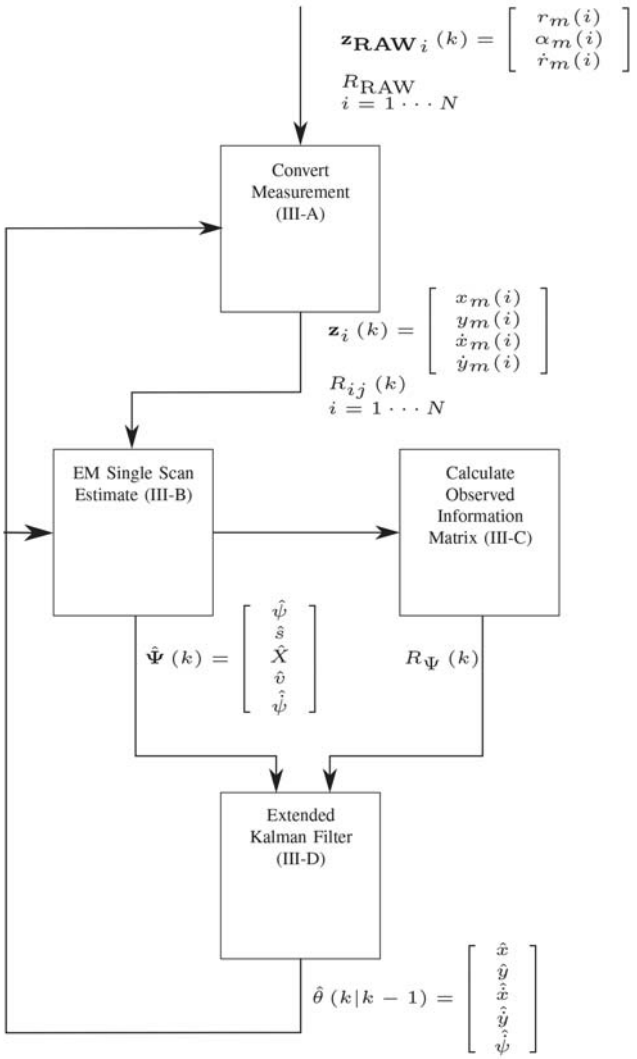

Fig. 1. Overview of the extended target tracking approach.

converted to Cartesian coordinates using the approach of [6]. These converted measurements are used in an EM algorithm for a single scan estimate of target position, size, heading, velocity and turn rate. The observed information matrix is calculated and used as a surrogate for the error covariance of this estimate. Finally, an extended Kalman filter with a coordinated turn motion model is used to combine the single scan estimates into a multi-scan estimate of the target state.

A. Measurement Conversion for an Individual Measurement

It is advantageous to first convert the raw measurements into Cartesian before processing. The raw measurements are converted into measurements of Cartesian position, x and y, and velocity, $\dot{x}$ and $\dot{y}$ using a simplified version of the method described in [6].

$$\mathbf{z}_i(k) = \begin{bmatrix} x_m(i,k) \\ y_m(i,k) \\ \dot{x}_m(i,k) \\ \dot{y}_m(i,k) \end{bmatrix} \tag{4}$$

$$= e^{\sigma_\alpha^2/2} \begin{bmatrix} r_m(i,k)\cos\alpha_m(i,k) \\ r_m(i,k)\sin\alpha_m(i,k) \\ \dot{r}_m(i,k)\cos\alpha_m(i,k) \\ \dot{r}_m(i,k)\sin\alpha_m(i,k) \end{bmatrix} \tag{5}$$

The conversion from range rate into Cartesian velocity assumes that the cross range rate is zero and accounts for any error in this assumption by setting the variance in the cross range rate dimension to infinity (or equivalently, setting the inverse to zero). This is implemented using the inverse converted measurement covariance, $R_{ij}(k)^{-1}$, which has a dimension of four by four, but is rank 3.

The converted measurement error covariance, $R_{ij}(k)$, is calculated according to Appendix A.

B. EM Single Scan Estimate from Multiple Measurements

1) Likelihood Model: Using the set of N measurements in combination with the target model, a single scan estimate of target position, size, heading, speed and turn rate can be calculated. The unknown parameters to be estimated form the vector $\mathbf{\Psi}$

$$\mathbf{\Psi} = [\mathbf{x}^{\mathrm{T}} \quad s \quad \psi \quad v \quad \dot{\psi}]^{\mathrm{T}} \tag{6}$$

The following probabilistic model is used for the likelihood function of $\mathbf{\Psi}$:

$$p_{\mathbf{z}}(\mathbf{z}_i \mid \mathbf{\Psi}) = \sum_{j=1}^{M} \pi_j p_{ij}(\mathbf{z}_i \mid \mathbf{\Psi}) \tag{7}$$

where, π_j is treated as the prior probability of a measurement originating from reflector j and $p_{\mathbf{z}}$ is the conditional probability density for a single measurement given $\mathbf{\Psi}$. This value is approximated using the probabilities of detection (ζ_j, $j = 1,\ldots,M$) by assuming each measurement comes from one of the reflectors, namely,

$$\pi_j = \frac{\zeta_j}{\sum_{l=1}^{M} \zeta_l} \tag{8}$$

The probability density function (pdf) for a given measurement-to-reflector combination, p_{ij} is given by

$$p_{ij}(\mathbf{z}_i \mid \mathbf{\Psi}) = |2\pi R_{ij}|^{-1/2} \cdot \{-\tfrac{1}{2}\nu_{ij}(\mathbf{\Psi},\mathbf{z}_i)^{\mathrm{T}} R_{ij}^{-1} \nu_{ij}(\mathbf{\Psi},\mathbf{z}_i)\} \tag{9}$$

where $\nu_{ij}(\mathbf{\Psi},\mathbf{z}_i)$, the difference between measurement i and reflector j, is

$$\nu_{ij}(\mathbf{\Psi},\mathbf{z}_i) = \mathbf{z}_i - \begin{bmatrix} sD(\psi)\mathbf{t}_j + \mathbf{x} \\ v\cos\psi - s\dot{\psi}|\mathbf{t}_j|\sin(\psi+\theta_j) \\ v\sin\psi + s\dot{\psi}|\mathbf{t}_j|\cos(\psi+\theta_j) \end{bmatrix} \tag{10}$$

where

$$D(\psi) = \begin{bmatrix} \cos\psi & -\sin\psi \\ \sin\psi & \cos\psi \end{bmatrix} \tag{11}$$

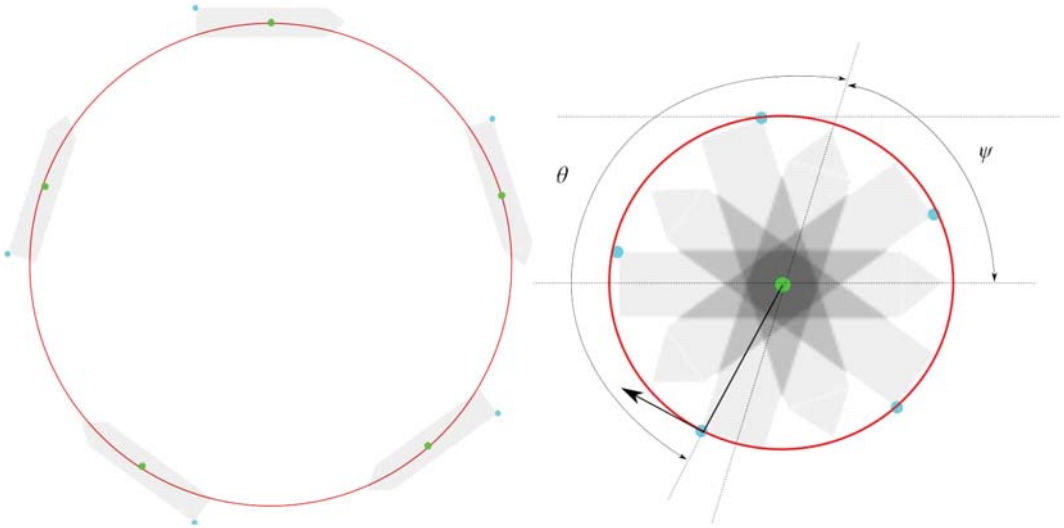

Fig. 2. Turn rate contribution to range rate.

is the rotation matrix,

$$|\mathbf{t}_j| = \sqrt{x_t(j)^2 + y_t(j)^2} \tag{12}$$

is the distance from reflector j to the target center,

$$\theta_j = \text{atan2}(y_t(j), x_t(j)) \tag{13}$$

is the angle of the line from the center to reflector j; relative to the reference direction, and R_{ij} is the converted measurement error covariance matrix (see appendix A).

The term $sD(\psi)\mathbf{t}_j + \mathbf{x}$ provides the position of target highlight j, scaled by the size, s, rotated by the heading ψ, and translated by the position of the target center $\mathbf{x}$.

In order to simultaneously estimate target speed (along its heading) and turn rate, the contribution of these terms to the measured instantaneous velocity must be separated. The terms $v\cos\psi$ and $v\sin\psi$ are the contributions of the target center's velocity to measured velocity. The terms $s\dot{\psi}|\mathbf{t}_j|\sin(\psi+\theta_j)$ and $s\dot{\psi}|\mathbf{t}_j|\cos(\psi+\theta_j)$ are the contributions due to turn rate. Fig. 2 shows the path of the target on the left [7]. When the motion of the target center is removed (as shown on the right), the motion of the individual highlights due to turn rate is evident.

The incomplete-data log-likelihood of $\mathbf{\Psi}$ based on all the measurements $\mathcal{Z}$ is given by [4]:

$$\begin{aligned}\ln\mathcal{L}(\mathbf{\Psi};\mathcal{Z}) &= \ln p_{\mathcal{Z}}(\mathcal{Z}\mid\mathbf{\Psi}) \\ &= \ln\prod_{i=1}^{N} p_{\mathbf{z}}(\mathbf{z}_i\mid\mathbf{\Psi}) \\ &= \sum_{i=1}^{N}\ln\left(\sum_{j=1}^{M}\pi_j p_{ij}(\mathbf{z}_i\mid\mathbf{\Psi},\mathbf{t}_j)\right)\end{aligned} \tag{14}$$

where $p_{\mathcal{Z}}$ is the conditional probability density of the set of measurements $\mathcal{Z}$, given $\mathbf{\Psi}$. For each measurement, $\mathbf{z}_i$, one has here the summation of its pdf if originated from reflector j and weighted by π_j.

2) Solving for $\mathbf{\Psi}$: To estimate $\mathbf{\Psi}$, one can find the vector that maximizes (14). The difficulty with (14) is the log of a sum. However, by recognizing (7) as a mixture model, the problem can be approached with the EM algorithm. The inside summation can be rewritten according to the EM approach using binary multipliers as missing data. The "missing" data are association variables that declare which reflector produced each measurement [16]. These association variables are expressed as binary vectors where each element in the binary vector corresponds to a reflector.

The binary vectors are defined as

$$\mathcal{Y} = [\mathbf{y}_1^{\mathrm{T}},\ldots,\mathbf{y}_N^{\mathrm{T}}]^{\mathrm{T}} \tag{15}$$

where $\mathbf{y}_i = [y_{i1},\ldots,y_{iM}]^{\mathrm{T}}$ is a M-dimensional binary vector (0 or 1), such that y_{ij} is one if measurement i is a reflection from reflector j, and zero otherwise. Each vector y_{ij} contains only one nonzero element. The complete log-likelihood, based also on $\mathcal{Y}$ is

$$\begin{aligned}\ln\mathcal{L}_{\mathrm{c}}(\mathbf{\Psi};\mathcal{Z},\mathcal{Y}) &= \ln p_{\mathrm{c}}(\mathcal{Z},\mathcal{Y}\mid\mathbf{\Psi}) \\ &= \sum_{i=1}^{N}\ln\left(\sum_{j=1}^{M} y_{ij}\pi_j p_{ij}(\mathbf{z}_i\mid\mathbf{\Psi})\right) \\ &= \sum_{i=1}^{N}\sum_{j=1}^{M} y_{ij}\ln(\pi_j p_{ij}(\mathbf{z}_i\mid\mathbf{\Psi}))\end{aligned} \tag{16}$$

where p_{c} is the conditional probability density of the complete data, $\mathcal{Z}$ and $\mathcal{Y}$, given $\mathbf{\Psi}$. If we view the missing data, $\mathcal{Y}$, as random variables, the EM $\mathcal{Q}$ function can now be found. In the EM algorithm, the $\mathcal{Q}$ function is iteratively maximized. This function is the expectation of the complete log-likelihood, with the expectation operation conducted with respect to the unknown data

$\mathcal{Y}$, given the observed data, $\mathcal{Z}$, and the estimate of $\boldsymbol{\Psi}$ from the previous iteration, $\boldsymbol{\Psi}^{(l)}$, namely,

$$\mathcal{Q}(\boldsymbol{\Psi};\boldsymbol{\Psi}^{(l)},\mathcal{Z}) = E\{\ln \mathcal{L}_c(\boldsymbol{\Psi};\mathcal{Z},\mathcal{Y}) \mid \mathcal{Z},\boldsymbol{\Psi}^{(l)}\} \tag{17}$$

$$\begin{aligned}\mathcal{Q}(\boldsymbol{\Psi};\boldsymbol{\Psi}^{(l)},\mathcal{Z}) &= \sum_{i=1}^{N}\sum_{j=1}^{M} w_{ij}(\boldsymbol{\Psi}^{(l)},\mathbf{z}_i)\ln(\pi_j p_{ij}(\mathbf{z}_i \mid \boldsymbol{\Psi})) \\ &= \sum_{i=1}^{N}\sum_{j=1}^{M} w_{ij}(\boldsymbol{\Psi}^{(l)},\mathbf{z}_i) \\ &\quad [\ln(\pi_j) - \tfrac{1}{2}\ln(|2\pi R_{ij}|) \\ &\quad - \tfrac{1}{2}\nu_{ij}(\boldsymbol{\Psi},\mathbf{z}_i)^{\mathrm{T}} R_{ij}^{-1}\nu_{ij}(\boldsymbol{\Psi},\mathbf{z}_i)]\end{aligned} \tag{18}$$

where w_{ij} is the estimate of the posterior association probabilities y_{ij} given the measurements and the previous estimate $\boldsymbol{\Psi}^{(l)}$, allowing for more than one measurement to be a reflection from a single reflector. Since this association model allows for more than one measurement to be a reflection from a single reflector, the model is an application of the PMHT association model [18]. The association probabilities are

$$\begin{aligned} w_{ij}(\boldsymbol{\Psi}^{(l)},\mathbf{z}_i) &= p_y(y_{ij} \mid \mathbf{z}_i,\boldsymbol{\Psi}^{(l)}) \\ &= \frac{\pi_j p_{ij}(\mathbf{z}_i \mid \boldsymbol{\Psi}^{(l)})}{\sum_{m=1}^{M}\pi_m p_{im}(\mathbf{z}_i \mid \boldsymbol{\Psi}^{(l)})}\end{aligned} \tag{19}$$

where p_y is the conditional probability of an association pair, given $\boldsymbol{\Psi}^{(l)}$ and measurement $\mathbf{z}_i$. The w_{ij} calculation given above assumes a clutter free environment. The extension to a cluttered environment is quite straightforward and simply requires an additional clutter distribution term in the denominator of the expression for w_{ij} [18] and the appropriate modification to $\mathcal{Y}$.

For the M step of EM, the $\mathcal{Q}$ function is maximized with respect to $\boldsymbol{\Psi}$. The $\boldsymbol{\Psi}$ that maximizes (18) can be found by solving

$$\nabla_{\boldsymbol{\Psi}}\mathcal{Q}(\boldsymbol{\Psi};\boldsymbol{\Psi}^{(l)},\mathcal{Z}) = 0 \tag{20}$$

to yield $\boldsymbol{\Psi}^{(l+1)}$, where

$$\begin{aligned}\nabla_{\boldsymbol{\Psi}}\mathcal{Q}(\boldsymbol{\Psi};\boldsymbol{\Psi}^{(l)},\mathcal{Z}) = -\frac{1}{2}\Bigg[\nabla_{\boldsymbol{\Psi}}\sum_{i=1}^{N}\sum_{j=1}^{M} w_{ij}(\boldsymbol{\Psi}^{(l)},\mathbf{z}_i) \\ \cdot \nu_{ij}(\boldsymbol{\Psi},\mathbf{z}_i)^{\mathrm{T}} R_{ij}^{-1}\nu_{ij}(\boldsymbol{\Psi},\mathbf{z}_i)\Bigg]\end{aligned} \tag{21}$$

Since R_{ij}^{-1} is symmetric and using

$$\nabla_{\mathbf{x}}\{f(\mathbf{x}^{\mathrm{T}})Af(\mathbf{x})\} = 2(\nabla_{\mathbf{x}}f(\mathbf{x}))^{\mathrm{T}}Af(\mathbf{x}) \tag{22}$$

one can simplify (21)

$$\begin{aligned}\nabla_{\boldsymbol{\Psi}}\mathcal{Q}(\boldsymbol{\Psi};\boldsymbol{\Psi}^{(l)},\mathcal{Z}) = -\sum_{i=1}^{N}\sum_{j=1}^{M} w_{ij}(\boldsymbol{\Psi}^{(l)},\mathbf{z}_i) \\ \cdot (\nu'_{ij}(\boldsymbol{\Psi}))^{\mathrm{T}} R_{ij}^{-1}\nu_{ij}(\boldsymbol{\Psi},\mathbf{z}_i)\end{aligned} \tag{23}$$

where

$$\nu'_{ij}(\boldsymbol{\Psi}) = \nabla_{\boldsymbol{\Psi}}\nu_{ij}(\boldsymbol{\Psi},\mathbf{z}_i) \tag{24}$$

The components of $\nu'_{ij}(\boldsymbol{\Psi})$ are

$$\nu'_{ij}(\boldsymbol{\Psi}) = -\begin{bmatrix} 1 & 0 & a_{13} & a_{14} & 0 & 0 \\ 0 & 1 & a_{23} & a_{24} & 0 & 0 \\ 0 & 0 & a_{33} & a_{34} & a_{35} & a_{36} \\ 0 & 0 & a_{34} & a_{44} & a_{45} & a_{46}\end{bmatrix} \tag{25}$$

where

$$\begin{bmatrix} a_{13} \\ a_{23} \\ a_{33} \\ a_{34}\end{bmatrix} = \begin{bmatrix} D(\psi)\mathbf{t}_j \\ -\dot{\psi}|\mathbf{t}_j|\sin(\psi+\theta_j) \\ \dot{\psi}|\mathbf{t}_j|\cos(\psi+\theta_j)\end{bmatrix} \tag{26}$$

$$\begin{bmatrix} a_{14} \\ a_{24} \\ a_{34} \\ a_{44}\end{bmatrix} = \begin{bmatrix} sD'(\psi)\mathbf{t}_j \\ -v\sin\psi - s\dot{\psi}|\mathbf{t}_j|\cos(\psi+\theta_j) \\ v\cos\psi - s\dot{\psi}|\mathbf{t}_j|\sin(\psi+\theta_j)\end{bmatrix} \tag{27}$$

$$\begin{bmatrix} a_{35} \\ a_{45}\end{bmatrix} = \begin{bmatrix}\cos\psi \\ \sin\psi\end{bmatrix} \tag{28}$$

$$\begin{bmatrix} a_{36} \\ a_{46}\end{bmatrix} = \begin{bmatrix} -s|\mathbf{t}_j|\sin(\psi+\theta_j) \\ s|\mathbf{t}_j|\cos(\psi+\theta_j)\end{bmatrix} \tag{29}$$

and

$$D'(\psi) = \begin{bmatrix} -\sin\psi & -\cos\psi \\ \cos\psi & -\sin\psi\end{bmatrix} \tag{30}$$

Since (20) cannot be solved directly, a first order Taylor expansion is used to find $\boldsymbol{\Psi}^{(l+1)}$, the maximizing $\boldsymbol{\Psi}$, given $\boldsymbol{\Psi}^{(l)}$, namely,

$$\begin{aligned}\sum_{i=1}^{N}\sum_{j=1}^{M} w_{ij}(\boldsymbol{\Psi}^{(l)},\mathbf{z}_i)\nu'_{ij}(\boldsymbol{\Psi})^{\mathrm{T}}R_{ij}^{-1} \\ \cdot [\nu_{ij}(\boldsymbol{\Psi},\mathbf{z}_i) + \nu'_{ij}(\boldsymbol{\Psi})(\boldsymbol{\Psi}^{(l+1)} - \boldsymbol{\Psi}^{(l)})] = 0\end{aligned} \tag{31}$$

which leads to

$$\begin{aligned}\boldsymbol{\Psi}^{(l+1)} &= \boldsymbol{\Psi}^{(l)} \\ &\quad + \left(\sum_{i=1}^{N}\sum_{j=1}^{M} w_{ij}(\boldsymbol{\Psi}^{(l)},\mathbf{z}_i)\nu'_{ij}(\boldsymbol{\Psi})^{\mathrm{T}}R_{ij}^{-1}\nu'_{ij}(\boldsymbol{\Psi})\right)^{-1} \\ &\quad \cdot \left(\sum_{i=1}^{N}\sum_{j=1}^{M} w_{ij}(\boldsymbol{\Psi}^{(l)},\mathbf{z}_i)\nu'_{ij}(\boldsymbol{\Psi})^{\mathrm{T}}R_{ij}^{-1}\nu_{ij}(\boldsymbol{\Psi},\mathbf{z}_i)\right)\Bigg|_{\boldsymbol{\Psi}^{(l)}}\end{aligned} \tag{32}$$

The resulting EM algorithm is defined as follows:

1) Initialize $\boldsymbol{\Psi}^{(l)}$
2) Calculate w using (19)
3) Solve for $\boldsymbol{\Psi}^{(l+1)}$ using (32).
4) Iteratively repeat steps 2 and 3 until a convergence criterion is met (e.g. when the increase in the complete log-likelihood is below a threshold).
5) Set $\hat{\boldsymbol{\Psi}}(k) = \boldsymbol{\Psi}^{(L)}$ at the last iteration, $l = L$.

C. Observed Information Matrix

In order to provide a measure of uncertainty for the estimate $\hat{\boldsymbol{\Psi}}$, critical information for tracking, the observed information matrix is used as a surrogate for the inverse covariance matrix. Oakes' formula [17] for the observed information matrix is used (see Appendix B).

$$-\nabla_{\boldsymbol{\Psi}}\nabla_{\boldsymbol{\Psi}}^{\mathrm{T}}\ln\mathcal{L}(\boldsymbol{\Psi};\mathcal{Z}) = -[\nabla_{\boldsymbol{\Psi}}\nabla_{\boldsymbol{\Psi}}^{\mathrm{T}}\mathcal{Q}(\boldsymbol{\Psi};\boldsymbol{\Psi}^{(L)},\mathcal{Z}) + \nabla_{\boldsymbol{\Psi}}\nabla_{\boldsymbol{\Psi}^{(L)}}^{\mathrm{T}}\mathcal{Q}(\boldsymbol{\Psi};\boldsymbol{\Psi}^{(L)},\mathcal{Z})] \tag{33}$$

Evaluating (33) using $\boldsymbol{\Psi} = \boldsymbol{\Psi}^{(L)}$ results in the "observed information matrix," $\boldsymbol{I}(\hat{\boldsymbol{\Psi}};\mathcal{Z})$ [16].

The first term on the right hand side of (33) is the observed information if the associations were known, $\boldsymbol{I}_c(\hat{\boldsymbol{\Psi}};\mathcal{Z})$:

$$\boldsymbol{I}_c(\hat{\boldsymbol{\Psi}};\mathcal{Z}) = -\nabla_{\boldsymbol{\Psi}}\nabla_{\boldsymbol{\Psi}}^{\mathrm{T}}\mathcal{Q}(\boldsymbol{\Psi};\boldsymbol{\Psi}^{(l)},\mathcal{Z}) \tag{34}$$

$$= -\sum_{i=1}^{N}\sum_{j=1}^{M} w_{ij}(\boldsymbol{\Psi}^{(l)},\mathbf{z}_i) \cdot [(\nu'_{ij}(\boldsymbol{\Psi}))^{\mathrm{T}}R_{ij}^{-1}\nu'_{ij}(\boldsymbol{\Psi}) + B_{ij}(\boldsymbol{\Psi},\mathbf{z}_i)] \tag{35}$$

where the B matrix is based on the second derivative of ν,

$$B_{ij}(\boldsymbol{\Psi},\mathbf{z}_i) = -\begin{bmatrix} 0 & 0 & 0 & 0 & 0 & 0 \\ 0 & 0 & 0 & 0 & 0 & 0 \\ 0 & 0 & 0 & b_{34} & 0 & b_{36} \\ 0 & 0 & b_{34} & b_{44} & b_{45} & b_{46} \\ 0 & 0 & 0 & b_{45} & 0 & 0 \\ 0 & 0 & b_{36} & b_{46} & 0 & 0 \end{bmatrix} \tag{36}$$

with components:

$$b_{34} = \begin{bmatrix} D'(\psi)\mathbf{t}_j \\ -\dot{\psi}|\mathbf{t}_j|\cos(\psi+\theta_j) \\ -\dot{\psi}|\mathbf{t}_j|\sin(\psi+\theta_j) \end{bmatrix}^{\mathrm{T}} R_{ij}^{-1}\nu_{ij}(\boldsymbol{\Psi},\mathbf{z}_i) \tag{37}$$

$$b_{36} = \begin{bmatrix} 0 \\ 0 \\ -|\mathbf{t}_j|\sin(\psi+\theta_j) \\ |\mathbf{t}_j|\cos(\psi+\theta_j) \end{bmatrix}^{\mathrm{T}} R_{ij}^{-1}\nu_{ij}(\boldsymbol{\Psi},\mathbf{z}_i) \tag{38}$$

$$b_{44} = \begin{bmatrix} -sD(\psi)\mathbf{t}_j \\ -v\cos\psi + s\dot{\psi}|\mathbf{t}_j|\sin(\psi+\theta_j) \\ -v\sin\psi - s\dot{\psi}|\mathbf{t}_j|\cos(\psi+\theta_j) \end{bmatrix}^{\mathrm{T}} R_{ij}^{-1}\nu_{ij}(\boldsymbol{\Psi},\mathbf{z}_i) \tag{39}$$

$$b_{45} = \begin{bmatrix} 0 \\ 0 \\ -\sin\psi \\ \cos\psi \end{bmatrix}^{\mathrm{T}} R_{ij}^{-1}\nu_{ij}(\boldsymbol{\Psi},\mathbf{z}_i) \tag{40}$$

$$b_{46} = \begin{bmatrix} 0 \\ 0 \\ -s|\mathbf{t}_j|\cos(\psi+\theta_j) \\ -s|\mathbf{t}_j|\sin(\psi+\theta_j) \end{bmatrix}^{\mathrm{T}} R_{ij}^{-1}\nu_{ij}(\boldsymbol{\Psi},\mathbf{z}_i) \tag{41}$$

The second term on the right hand side of (33) accounts for the association uncertainty, $\boldsymbol{I}_m(\hat{\boldsymbol{\Psi}};\mathcal{Z})$. This is found by taking the derivative of $\mathcal{Q}$ with respect to $\boldsymbol{\Psi}$, and taking the derivative with respect to $\boldsymbol{\Psi}^{(L)^{\mathrm{T}}}$, i.e.

$$\boldsymbol{I}_m(\hat{\boldsymbol{\Psi}};\mathcal{Z}) = -\nabla_{\boldsymbol{\Psi}}\nabla_{\boldsymbol{\Psi}^{(L)}}^{\mathrm{T}}\mathcal{Q}(\boldsymbol{\Psi};\boldsymbol{\Psi}^{(L)},\mathcal{Z}) = -\sum_{i=1}^{N}\sum_{j=1}^{M} w'_{ij}(\boldsymbol{\Psi}^{(L)},\mathbf{z}_i)(\nu'_{ij}(\boldsymbol{\Psi}))^{\mathrm{T}}R_{ij}^{-1}\nu_{ij}(\boldsymbol{\Psi},\mathbf{z}_i) \tag{42}$$

where w' is the derivative of (19)

$$w'_{ij}(\boldsymbol{\Psi}^{(L)},\mathbf{z}_i) = \pi_j p_{ij}(\mathbf{z}_i \mid \boldsymbol{\Psi}^{(L)}) \left\{ \left(\sum_{m=1}^{M} \pi_m p_{im}(\mathbf{z}_i \mid \boldsymbol{\Psi}^{(L)}) \right)^{-2} \cdot \sum_{m=1}^{M} [\pi_m p_{im}(\mathbf{z}_i \mid \boldsymbol{\Psi}^{(L)}) \cdot (\nu'_{im}(\boldsymbol{\Psi}^{(L)}))^{\mathrm{T}}R_{im}^{-1}\nu_{im}(\boldsymbol{\Psi}^{(L)},\mathbf{z}_i)] - \frac{(\nu'_{ij}(\boldsymbol{\Psi}^{(L)}))^{\mathrm{T}}R_{ij}^{-1}\nu_{ij}(\boldsymbol{\Psi}^{(L)},\mathbf{z}_i)}{\sum_{m=1}^{M}\pi_m p_{im}(\mathbf{z}_i \mid \boldsymbol{\Psi}^{(L)})} \right\} \tag{43}$$

D. Extended Kalman Filter for Multi-Scan Estimation

The single scan estimate of the target state can be used in an EKF to provide multi-scan estimates. The EKF for a coordinated turn motion model is well known for the case of position only measurements (pp. 466–470 of [1]). The state vector for the CT-EKF is

$$\hat{\boldsymbol{\theta}} = [x_{\hat{\theta}} \quad \dot{x}_{\hat{\theta}} \quad y_{\hat{\theta}} \quad \dot{y}_{\hat{\theta}} \quad \dot{\psi}_{\hat{\theta}}]^{\mathrm{T}} \tag{44}$$

Note that the subscript $\hat{\boldsymbol{\theta}}$ is used to avoid confusion between the elements of $\hat{\boldsymbol{\theta}}$ and $\boldsymbol{\Psi}$.

The dynamic equation is

$$\boldsymbol{\theta}(k+1) = f[k,\boldsymbol{\theta}(k)] + \Gamma(k)\upsilon(k) \tag{45}$$

and the state prediction is:

$$\hat{\boldsymbol{\theta}}(k+1 \mid k) = f[k,\hat{\boldsymbol{\theta}}(k \mid k)] \tag{46}$$

where $f[k,\hat{\boldsymbol{\theta}}(k \mid k)]$ is:

$$\begin{bmatrix} 1 & \frac{\sin(\dot{\psi}_{\hat{\theta}}(k)T)}{\dot{\psi}_{\hat{\theta}}(k)} & 0 & -\frac{1-\cos(\dot{\psi}_{\hat{\theta}}(k)T)}{\dot{\psi}_{\hat{\theta}}(k)} & 0 \\ 0 & \cos(\dot{\psi}_{\hat{\theta}}(k)T) & 0 & -\sin(\dot{\psi}_{\hat{\theta}}(k)T) & 0 \\ 0 & \frac{1-\cos(\dot{\psi}_{\hat{\theta}}(k)T)}{\dot{\psi}_{\hat{\theta}}(k)} & 1 & \frac{\sin(\dot{\psi}_{\hat{\theta}}(k)T)}{\dot{\psi}_{\hat{\theta}}(k)} & 0 \\ 0 & \sin(\dot{\psi}_{\hat{\theta}}(k)T) & 0 & \cos(\dot{\psi}_{\hat{\theta}}(k)T) & 0 \\ 0 & 0 & 0 & 0 & 1 \end{bmatrix} \hat{\boldsymbol{\theta}}(k \mid k) \tag{47}$$

and

$$\Gamma(k) = \begin{bmatrix} \frac{1}{2}T^2 & 0 & 0 \\ T & 0 & 0 \\ 0 & \frac{1}{2}T^2 & 0 \\ 0 & T & 0 \\ 0 & 0 & T \end{bmatrix} \tag{48}$$

The state prediction covariance is:

$$P(k+1 \mid k) = F(k)P(k \mid k)F(k)^{\mathrm{T}} + \Gamma(k)Q(k)\Gamma(k)^{\mathrm{T}} \tag{49}$$

where Q is the covariance of the process noise, υ, and

$$F(k) = \left.\frac{\partial f(k)}{\partial \boldsymbol{\theta}}\right|_{\boldsymbol{\theta}=\hat{\boldsymbol{\theta}}(k+1|k)} \tag{50}$$

Two modifications to the CT-EKF in [1] are necessary for this application. This first is in the observation function. Using the single scan estimate, $\hat{\boldsymbol{\Psi}}$, as the observation, the full state vector can be observed, thus eliminating the need for an observation matrix (commonly referred to as the H matrix, i.e., here H is the identity matrix). The single scan observation, $\mathbf{z}_{\mathrm{C}}$ and the inverse observation error covariance, R_{C}^{-1}, are:

$$\mathbf{z}_{\mathrm{C}}(k) = \begin{bmatrix} 1 & 0 & 0 & 0 & 0 & 0 \\ 0 & 0 & 0 & 0 & \cos\psi & 0 \\ 0 & 1 & 0 & 0 & 0 & 0 \\ 0 & 0 & 0 & 0 & \sin\psi & 0 \\ 0 & 0 & 0 & 0 & 0 & 1 \end{bmatrix} \boldsymbol{\Psi}(k) \tag{51}$$

$$R_{\mathrm{C}}(k)^{-1} = (A^{-1})^{\mathrm{T}} \boldsymbol{I}(\hat{\boldsymbol{\Psi}}; \mathcal{Z}) A^{-1} \tag{52}$$

where $\boldsymbol{I}(\hat{\boldsymbol{\Psi}}; \mathcal{Z})$ was defined following (33).

$$A = \begin{bmatrix} 1 & 0 & 0 & 0 & 0 & 0 \\ 0 & 0 & 0 & 0 & -\sin\psi & 0 \\ 0 & 1 & 0 & 0 & 0 & 0 \\ 0 & 0 & 0 & 0 & \cos\psi & 0 \\ 0 & 0 & 0 & 0 & 0 & 1 \end{bmatrix} \tag{53}$$

A second modification is required since R_{C}^{-1} is not necessarily invertible. The inverse error covariance matrices for the individual measurements, R_{ij}^{-1}, are not invertible due to the fact that the information related to cross range velocity is zero (it has a zero eigenvalue in the cross range rate direction). Although, R_{C}^{-1} will be invertible for most scans, it is not invertible if the target aspect is 90°, or if there is only one measurement in the scan. To allow for this possibility, the information form of the EKF is utilized. The EKF update is:

$$W(k+1) = [P(k+1 \mid k)^{-1} + R_{\mathrm{C}}(k+1)^{-1}]^{-1} \cdot R_{\mathrm{C}}(k+1)^{-1} \tag{54}$$

$$P(k+1 \mid k+1) = [P(k+1 \mid k)^{-1} + R_{\mathrm{C}}(k+1 \mid k)^{-1}]^{-1} \tag{55}$$

$$\hat{\boldsymbol{\theta}}(k+1 \mid k+1) = \hat{\boldsymbol{\theta}}(k+1 \mid k) + W(k+1) \cdot [\mathbf{z}_{\mathrm{C}}(k) - \hat{\boldsymbol{\theta}}(k+1 \mid k)] \tag{56}$$

IV. IMPLEMENTATION AND RESULTS

A. Implementation

1) EM Initialization: As with any optimization approach, care must be taken when employing the algorithm during initialization to avoid convergence to a local maximum. The initialization approach chosen here is as follows.

The initial value for $\mathbf{x}^{(0)}$ is simply the mean of all the position measurements. The initial value for size, $s^{(0)}$, is set to the ratio of the average distance from the measurement to $\mathbf{x}^{(0)}$ and the average distance of the target highlight, $\mathbf{t}$, to the target center. The initial value for heading, $\psi^{(0)}$, is calculated by finding the covariance of the position measurements and estimating the heading based on the largest eigenvector. The initial speed and turn rate are set to 0.

A particular concern for local maximums for many target models is one at a heading of 180 degrees from the true heading. To avoid maximizing at this incorrect heading, the algorithm is optimized using two initial headings, 180 degrees apart, and the result with the highest likelihood is used.

Even with proper initialization, converging to a local instead of global maximum is a concern. To help, the R matrix is artificially inflated for the first few iterations of the algorithm. This tends to smooth the likelihood surface. Optimization on the augmented surface first reduces the probability of converging to a local maximum. This approach is related to the deterministic annealing EM algorithm [19].

2) Limitations: It is important to note the limitations of the algorithm in its ability to estimate velocity and turn rate. Regardless of the target model, the ability to estimate velocity from range rate measurements will be limited when the target is traveling across the line of sight from the sensor. Turn rate estimation will also be limited for targets that do not have significant width when the target is traveling directly towards or away from the sensor. To analyze these effects the Cramer-Rao low bound (CRLB) is examined for two target types. Evident in (33) is that the CRLB is a function of the measurements. The looser bound of (35) is used here and is calculated using the expected measurement. The bound provides a lower bound on the average square

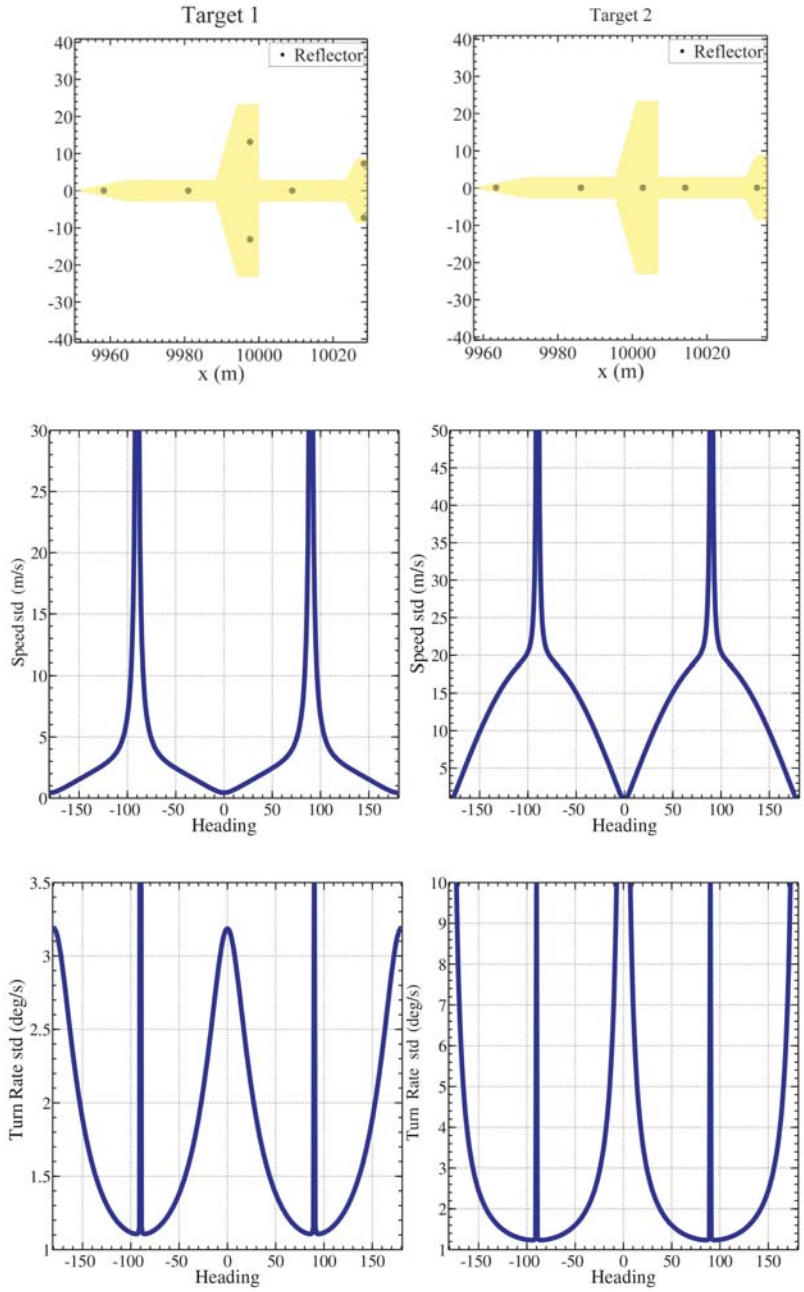

Fig. 3. CRLB analysis (using (35)) for a target that has width (target 1) and one without width (target 2).

error, but is looser than the CRLB due to the fact that it does not consider assignment uncertainty. Nevertheless, this bound is sufficient to demonstrate the limitations in the algorithm at various aspect angles. For this test the heading was varied from -180 to 180 degrees, the probability of detection was set to 1, the size was set to 70 m, position set to $[10\ \ 0]^{\mathrm{T}}$ km, the speed set 120 m/s and the turn-rate set to 3 deg/sec. The measurement error covariance was set as follows:

1) $\sigma_r = 2$ m
2) $\sigma_{\dot{r}} = 1$ m/s
3) $\sigma_{\alpha} = 0.05$ deg
4) $\rho\sigma_r\sigma_{\dot{r}} = 0$

As seen from Figure 3, if the target has width then turn-rate and speed can be estimated at all aspects with the exception of $+/-90$ degrees. In the case of a line-like target, such as target 2 in Figure 3, speed can be estimated at all aspects with the exception of aspects near $+/-90$ degrees, while turn-rate cannot be estimated at $+/-90$ degrees and near 0 or 180 degrees.

3) Implementation Details: There are three notable implementation details that are required for robust performance of the algorithm. The first is dealing with the inability to estimate velocity when the target aspect is 90 deg. Since the true error covariance of the single scan estimate is unknown, the observed information matrix serves as a surrogate. When the true target aspect is

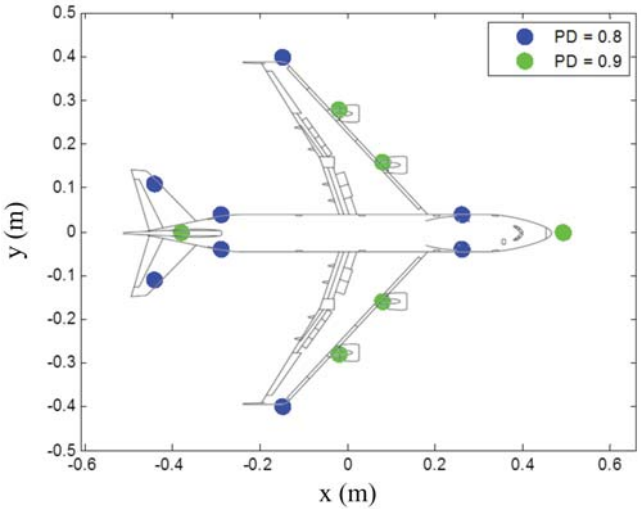

Fig. 4. Target template

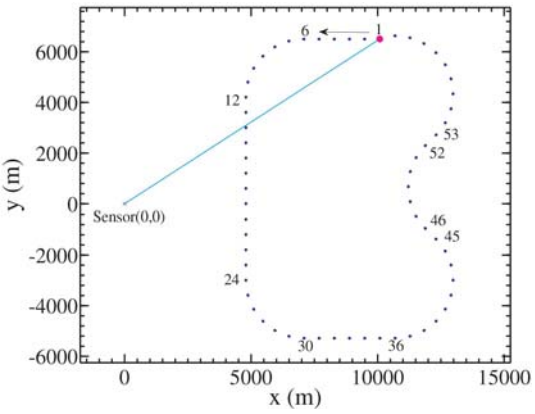

Fig. 5. Target path for the test case. The position of the target at each scan is shown. The first scan, as well as any scan that is starting a maneuver is labeled. The sensor position is at the origin. The line-of-sight for the first scan is also shown.

90 deg, while the observed aspect is near, but not equal to 90, the observed information matrix will be overconfident in the velocity estimate. To avoid this, when the estimated aspect, based on $\hat{\theta}(k+1 \mid k)$, is near 90 degrees, the velocity estimate should not be used. This is achieved by setting the appropriate rows and columns of $R_{\mathrm{C}}(k)^{-1}$ to zero. (For targets with little or no width, a similar test is required for turn-rate estimation at aspects near 0 or 180 deg.)

A related issue is that when the estimated target aspect is close to 90 deg, components of $R_{\mathrm{C}}(k)^{-1}$ may be close to zero, resulting in a badly conditioned matrix. In these cases, only the position portion of the single scan estimate is used. (Note that the first issue occurs when the true target aspect is 90 deg, while the second issue is when the estimated target aspect is close to 90 deg).

Finally, since the EM algorithm may converge on a local maximum, gating is used to validate the single scan estimate based on the innovation in the EKF update. If the innovation for either the velocity or turn-rate is too large, only the position portion of the single scan estimate is used. Again, this is achieved by setting the appropriate rows and columns of $R_{\mathrm{C}}(k)^{-1}$ to zero.

B. Results

The new algorithm was tested in a aircraft tracking application. The target template is based on a commercial airliner (see Fig. 4), with probability of detections for the highlights at 0.8 and 0.9. The aircraft follows the path shown in Fig. 5. The measurement error covariance was set the same as Section IV-A.2. The EKF is implemented assuming the following process noise:

$$Q = \begin{bmatrix} (0.25)^2 & 0 & 0 \\ 0 & (0.25)^2 & 0 \\ 0 & 0 & \left(0.6\frac{\pi}{180}\right)^2 \end{bmatrix} \tag{57}$$

Fig. 6 shows the average normalized estimation error squared (ANEES) [1] and mean square error for position, velocity and turn rate. Errors are shown for the state prediction ($\hat{\theta}(k \mid k-1)$) for the algorithm (EXTGTEKF). Since the primary advantage of the proposed algorithm is the exploitation of the target shape to extract speed and turn rate, a tracker that does not extract these quantities is used for comparison (POSEKF). The POSEKF is identical to the EXTGTEKF, with the important exception that only the position portion of the observation, $\mathbf{z}_{\mathrm{C}}$, is used. This is achieved by setting the appropriate rows and columns of $R_{\mathrm{C}}(k)^{-1}$ to zero. The proposed algorithm exhibits better consistency (ANEES closer to 1) and, in general, improved mean square error (MSE). Unlike the POSEKF algorithm, the EXTGTEKF does not lag in the turn-rate estimate since turn-rate is measured directly. The turn rate estimate for the EXTGTEKF is significantly better when the turn initiates, but it worse in steady state. This is due to the fact that the turn rate estimate for the POSEKF requires three position measurements, resulting in a smoother estimate. It is a trade-off between lag and smoothing. Performance of the EXTGTEKF is, as expected, degraded for target aspects near 90 deg. (e.g. near scan 19), as the EXTGTEKF reverts to position only measurements during those periods.

V. CONCLUSION

A novel approach to extended object tracking has been presented. A target model has been developed for the target spatial characteristics that is appropriate for estimation, flexible enough to handle various target types, and loose enough such that exact knowledge of the target size is not required. By restricting the spatial characteristics to be fixed with respect to the line of motion, the resulting algorithm allows for single scan estimation of position, heading, size, velocity and turn rate by using measurements of position and range rate. These single scan measurements when used in a multi-scan tracking algorithm (i.e. extended Kalman filter) provide improved estimates of target position, velocity

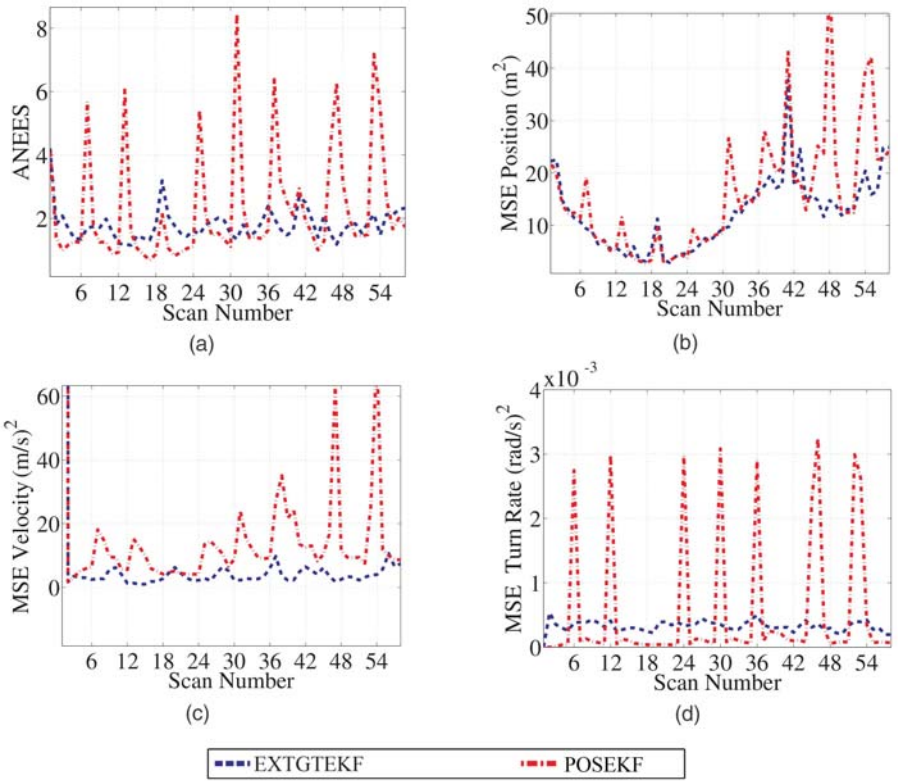

Fig. 6. Results of a 500 run Monte Carlo evaluation of the estimated state for the new EXTGTEKF and a position-only cluster tracker (CLUSTEREKF). a. Average Normalized Estimation Error Squared (ANEES). b. Mean Square Error (MSE) for Position Estimate. c. Mean Square Error (MSE) for Velocity Estimate. d. Mean Square Error (MSE) for Turn Rate Estimate.

and turn rate compared to a traditional cluster tracker using only position measurements. A primary advantage is that the new method, unlike methods using only position measurements, does not suffer from a lag in the estimation of turn rate and the resulting estimation errors.

APPENDIX A CONVERTED MEASUREMENT ERROR COVARIANCE

The converted measurement error covariance is approximated using a simplification of [6]. The calculation requires a prediction, which is based on the one step prediction, $\hat{\boldsymbol{\theta}}(k \mid k-1)$. Using this prediction, in combination with the target template and the previous estimate of the size, s, the state of an individual highlight can be calculated (which will be referred to as $\mathbf{x}_j$).

First the predicted highlight state is rotated into the estimate's line of sight (LOS) coordinate system. Noting that the inverse of the direction cosine matrix, $D(\alpha_m)$, is its transpose, the rotated state is calculated as:

$$\hat{\mathbf{x}}_{\mathrm{R}} = D(\alpha_t)^{\mathrm{T}}\hat{\mathbf{x}}_j \tag{58}$$

where the predicted bearing to the highlight is

$$\alpha_t = \tan^{-1}\left(\frac{\hat{\mathbf{x}}^2_{k+1|k}}{\hat{\mathbf{x}}^1_{k+1|k}}\right) \tag{59}$$

and $\hat{\mathbf{x}}^n$ is the nth component of $\hat{\mathbf{x}}$.

$$R_{\mathrm{R}}^{11} = \tfrac{1}{2}[(\hat{\mathbf{x}}_{\mathrm{R}}^1)^2 + \sigma_r^2](1 + e^{-2\sigma_\alpha^2})e^{\sigma_\alpha^2} - (\hat{\mathbf{x}}_{\mathrm{R}}^1)^2 \tag{60}$$

$$R_{\mathrm{R}}^{12} = 0 \tag{61}$$

$$R_{\mathrm{R}}^{13} = \tfrac{1}{2}(\hat{\mathbf{x}}_{\mathrm{R}}^1\hat{\mathbf{x}}_{\mathrm{R}}^3 + \rho\sigma_r\sigma_{\dot{r}})(1 + e^{-2\sigma_\alpha^2})e^{\sigma_\alpha^2} - \hat{\mathbf{x}}_{\mathrm{R}}^1\hat{\mathbf{x}}_{\mathrm{R}}^3 \tag{62}$$

$$R_{\mathrm{R}}^{22} = \tfrac{1}{2}[(\hat{\mathbf{x}}_{\mathrm{R}}^1)^2 + \sigma_r^2](1 - e^{-2\sigma_\alpha^2})e^{\sigma_\alpha^2} \tag{63}$$

$$R_{\mathrm{R}}^{23} = \tfrac{1}{2}(\hat{\mathbf{x}}_{\mathrm{R}}^1\hat{\mathbf{x}}_{\mathrm{R}}^4)(1 - e^{-2\sigma_\alpha^2})e^{\sigma_\alpha^2} \tag{64}$$

$$R_{\mathrm{R}}^{33} = \tfrac{1}{2}[(\hat{\mathbf{x}}_{\mathrm{R}}^3)^2 + \sigma_r^2](1 + e^{-2\sigma_\alpha^2})e^{\sigma_\alpha^2} - (\hat{\mathbf{x}}_{\mathrm{R}}^3)^2 + \tfrac{1}{2}[(\hat{\mathbf{x}}_{\mathrm{R}}^4)^2 + \sigma_{\dot{c}}^2](1 - e^{-2\sigma_\alpha^2})e^{\sigma_\alpha^2} \tag{65}$$

Since the cross range rate measurement, $\dot{c}_m$, is non-informative, its standard deviation, $\sigma_{\dot{c}}$, is infinite. One can, however, set the value of $\sigma_{\dot{c}}$ used in (65) based on an a priori estimate of the standard deviation of target cross range rate to capture the effect that the cross range rate has on the ability to measure the line of sight velocity. The remaining components of the measurement noise covariance in the coordinate system, R_{R} (e.g. R_{R}^{44}, R_{R}^{34}), are are set to infinity to capture that $\dot{c}_m$ is non-informative. It is therefore useful to deal with the inverse of R_{R} and note that for a positive definite covariance matrix,

$$\left.\begin{bmatrix} \sigma_1^2 & \rho\sigma_1\sigma_2 \\ \rho\sigma_1\sigma_2 & \sigma_2^2 \end{bmatrix}^{-1}\right|_{\sigma_2\to\infty} = \begin{bmatrix} (\sigma_1^2)^{-1} & 0 \\ 0 & 0 \end{bmatrix} \tag{66}$$

therefore

$$R_{\mathrm{R}}^{-1} = \begin{bmatrix} & & & 0 \\ & (R_{\mathrm{R}}^{1:3,1:3})^{-1} & & 0 \\ & & & 0 \\ 0 & 0 & 0 & 0 \end{bmatrix} \tag{67}$$

The measurement noise covariance for (5), R_{ij}, is

$$R_{ij}^{-1} = D(\alpha_t) R_{\mathrm{R}}^{-1} D(\alpha_t)^{\mathrm{T}} \tag{68}$$

Since R_{C}^{-1} is not invertible, R_{ij} is not available for use in the Kalman filter gain calculation; one has to use the information form of the Kalman filter. The determinant of R_{ij} (needed for (9) in the calculation of w_{ij} using (19)) is also not available, so the determinant of R_{R} is used as a surrogate.

This is a simplification of (35)–(38) in [6]. The simplification is warranted due to the more accurate measurement in the present manuscript when compared to the measurement accuracy of [6].

APPENDIX B OAKES' FORMULA

In [17], a simple explicit formula is given for the observed information matrix. A summary of Oakes' work is provided below with the necessary background from [8].

$$\begin{aligned} \mathcal{L}(\boldsymbol{\Psi}; \mathcal{Z}) &= p_{\mathcal{Z}}(\mathcal{Z} \mid \boldsymbol{\Psi}) \\ &= \frac{p_{\mathrm{c}}(\mathcal{Z}, \mathcal{Y} \mid \boldsymbol{\Psi}) p_{\mathcal{Z}}(\mathcal{Z} \mid \boldsymbol{\Psi})}{p_{\mathrm{c}}(\mathcal{Z}, \mathcal{Y} \mid \boldsymbol{\Psi})} \end{aligned} \tag{69}$$

where $p_{\mathrm{c}}(\mathcal{Z}, \mathcal{Y} \mid \boldsymbol{\Psi})$ is defined after (16). Let $k(\mathcal{X} \mid \mathcal{Z}, \boldsymbol{\Psi})$ be the conditional probability of the complete data, $\mathcal{X}$, given the observed data, $\mathcal{Z}$, namely

$$k(\mathcal{X} \mid \mathcal{Z}, \boldsymbol{\Psi}) = \frac{p_{\mathrm{c}}(\mathcal{Z}, \mathcal{Y} \mid \boldsymbol{\Psi})}{p_{\mathcal{Z}}(\mathcal{Z} \mid \boldsymbol{\Psi})} \tag{70}$$

Therefore

$$\mathcal{L}(\boldsymbol{\Psi}; \mathcal{Z}) = \frac{p_{\mathrm{c}}(\mathcal{Z}, \mathcal{Y} \mid \boldsymbol{\Psi})}{k(\mathcal{X} \mid \mathcal{Z}, \boldsymbol{\Psi})} \tag{71}$$

and

$$\ln \mathcal{L}(\boldsymbol{\Psi}; \mathcal{Z}) = \ln p_{\mathrm{c}}(\mathcal{Z}, \mathcal{Y} \mid \boldsymbol{\Psi}) - \ln k(\mathcal{X} \mid \mathcal{Z}, \boldsymbol{\Psi}) \tag{72}$$

Taking the expectation of both sides with respect to the conditional distribution of $\mathcal{X}$ given $\mathcal{Z}$, using the previous estimate $\boldsymbol{\Psi}^{(l)}$ for $\boldsymbol{\Psi}$ gives

$$\begin{aligned} \ln \mathcal{L}(\boldsymbol{\Psi}; \mathcal{Z}) &= E\{\ln \mathcal{L}_{\mathrm{c}}(\boldsymbol{\Psi}; \mathcal{Z}, \mathcal{Y}) \mid \mathcal{Z}, \boldsymbol{\Psi}^{(l)}\} \\ &\quad - E\{\ln k(\mathcal{X} \mid \mathcal{Z}, \boldsymbol{\Psi}) \mid \mathcal{Z}, \boldsymbol{\Psi}^{(l)}\} \\ &= \mathcal{Q}(\boldsymbol{\Psi}; \boldsymbol{\Psi}^{(l)}, \mathcal{Z}) - H(\boldsymbol{\Psi}; \boldsymbol{\Psi}^{(l)}, \mathcal{Z}) \end{aligned} \tag{73}$$

using (17) and where

$$H(\boldsymbol{\Psi}; \boldsymbol{\Psi}^{(l)}, \mathcal{Z}) = E\{\ln k(\mathcal{X} \mid \mathcal{Z}, \boldsymbol{\Psi}) \mid \mathcal{Z}, \boldsymbol{\Psi}^{(l)}\} \tag{74}$$

In [8] the following is shown using Jensen's inequality,

$$H(\boldsymbol{\Psi}; \boldsymbol{\Psi}^{(l)}, \mathcal{Z}) \leq H(\boldsymbol{\Psi}^{(l)}; \boldsymbol{\Psi}^{(l)}, \mathcal{Z}) \tag{75}$$

for all $\boldsymbol{\Psi}$ in the parameter space. This is fundamental in the proof for EM convergence, and leads to

$$\nabla_{\boldsymbol{\Psi}} H(\boldsymbol{\Psi}; \boldsymbol{\Psi}^{(l)}, \mathcal{Z})|_{\boldsymbol{\Psi} = \boldsymbol{\Psi}^{(l)}} = 0 \tag{76}$$

Assuming that the expectation with respect to $\mathcal{X}$ and differentiation with respect to $\boldsymbol{\Psi}$ are interchangeable,

$$E\{\nabla_{\boldsymbol{\Psi}} \ln k(\mathcal{X} \mid \mathcal{Z}, \boldsymbol{\Psi}) \mid \mathcal{Z}, \boldsymbol{\Psi}^{(l)}\} = 0 \tag{77}$$

Also, from equivalent statements of Fisher's information,

$$\begin{aligned} &- E\{\nabla_{\boldsymbol{\Psi}} \nabla_{\boldsymbol{\Psi}}^{\mathrm{T}} \ln k(\mathcal{X} \mid \mathcal{Z}, \boldsymbol{\Psi}) \mid \mathcal{Z}, \boldsymbol{\Psi}^{(l)}\} \\ &\quad = E\{\nabla_{\boldsymbol{\Psi}} k(\mathcal{X} \mid \mathcal{Z}, \boldsymbol{\Psi}) \nabla_{\boldsymbol{\Psi}} k(\mathcal{X} \mid \mathcal{Z}, \boldsymbol{\Psi})^{\mathrm{T}} \mid \mathcal{Z}, \boldsymbol{\Psi}^{(l)}\} \end{aligned} \tag{78}$$

Differentiation of (73) with respect to $\boldsymbol{\Psi}$ gives

$$\begin{aligned} \nabla_{\boldsymbol{\Psi}} \ln \mathcal{L}(\boldsymbol{\Psi}; \mathcal{Z}) &= \nabla_{\boldsymbol{\Psi}} \mathcal{Q}(\boldsymbol{\Psi}; \boldsymbol{\Psi}^{(l)}, \mathcal{Z}) \\ &\quad - E\{\nabla_{\boldsymbol{\Psi}} \ln k(\mathcal{X} \mid \mathcal{Z}, \boldsymbol{\Psi}) \mid \mathcal{Z}, \boldsymbol{\Psi}^{(l)}\} \end{aligned} \tag{79}$$

By evaluating (79) using $\boldsymbol{\Psi}^{(l)} = \boldsymbol{\Psi}$ and noting (77), we obtain

$$\nabla_{\boldsymbol{\Psi}} \ln \mathcal{L}(\boldsymbol{\Psi}; \mathcal{Z}) = \nabla_{\boldsymbol{\Psi}} \mathcal{Q}(\boldsymbol{\Psi}; \boldsymbol{\Psi}^{(l)}, \mathcal{Z})|_{\boldsymbol{\Psi}^{(l)} = \boldsymbol{\Psi}} \tag{80}$$

Differentiation of (79) with respect to $\boldsymbol{\Psi}$ gives,

$$\begin{aligned} &\nabla_{\boldsymbol{\Psi}} \nabla_{\boldsymbol{\Psi}}^{\mathrm{T}} \ln \mathcal{L}(\boldsymbol{\Psi}; \mathcal{Z}) \\ &\quad = \nabla_{\boldsymbol{\Psi}} \nabla_{\boldsymbol{\Psi}}^{\mathrm{T}} \mathcal{Q}(\boldsymbol{\Psi}; \boldsymbol{\Psi}^{(l)}, \mathcal{Z}) \\ &\quad\quad - E\{\nabla_{\boldsymbol{\Psi}} \nabla_{\boldsymbol{\Psi}}^{\mathrm{T}} \ln k(\mathcal{X} \mid \mathcal{Z}, \boldsymbol{\Psi}) \mid \mathcal{Z}, \boldsymbol{\Psi}^{(l)}\} \end{aligned} \tag{81}$$

Differentiation of (79) with respect to $\boldsymbol{\Psi}^{(l)}$ gives,

$$\begin{aligned} \mathbf{0} &= \nabla_{\boldsymbol{\Psi}} \nabla_{\boldsymbol{\Psi}^{(l)}{}^{\mathrm{T}}} \mathcal{Q}(\boldsymbol{\Psi}; \boldsymbol{\Psi}^{(l)}, \mathcal{Z}) \\ &\quad - E\{\nabla_{\boldsymbol{\Psi}} \ln k(\mathcal{X} \mid \mathcal{Z}, \boldsymbol{\Psi}) \nabla_{\boldsymbol{\Psi}^{(l)}} \ln k(\mathcal{X} \mid \mathcal{Z}, \boldsymbol{\Psi})^{\mathrm{T}} \mid \mathcal{Z}, \boldsymbol{\Psi}^{(l)}\} \end{aligned} \tag{82}$$

where $\mathbf{0}$ is the appropriately sized null matrix.

Substitution $\boldsymbol{\Psi} = \boldsymbol{\Psi}^{(l)}$ and adding (81) and (82) results in

$$\begin{aligned} \nabla_{\boldsymbol{\Psi}} \nabla_{\boldsymbol{\Psi}}^{\mathrm{T}} \ln \mathcal{L}(\boldsymbol{\Psi}; \mathcal{Z}) &= \nabla_{\boldsymbol{\Psi}} \nabla_{\boldsymbol{\Psi}}^{\mathrm{T}} \mathcal{Q}(\boldsymbol{\Psi}; \boldsymbol{\Psi}^{(l)}, \mathcal{Z}) \\ &\quad + \nabla_{\boldsymbol{\Psi}} \nabla_{\boldsymbol{\Psi}^{(l)}}^{\mathrm{T}} \mathcal{Q}(\boldsymbol{\Psi}; \boldsymbol{\Psi}^{(l)}, \mathcal{Z}) \end{aligned} \tag{83}$$

This result is used in (33), using the $\boldsymbol{\Psi}^{(l)}$ from the last EM iteration for a scan (i.e. $\boldsymbol{\Psi}^{(L)}$).

ACKNOWLEDGMENT

Steven Bordonaro was supported by ONR Independent Applied Research (IAR). Peter Willett was supported by ONR under contract N00014-13-1-0231. Yaakov Bar-Shalom was supported under ARO W991NF-10-1-0369.

REFERENCES

[1] Y. Bar-Shalom, X. R. Li, and T. Kirubarajan
Estimation with Applications to Tracking and Navigation. New York & Boston: John Wiley and Sons, 2001.

[2] M. Baum and U. Hanebeck
"Shape tracking of extended objects and group targets with star-convex RHMs,"
in *Proceedings of the 14th International Conference on Information Fusion (FUSION)*. IEEE, 2011, pp. 1–8.

[3] M. Baum, B. Noack, and U. Hanebeck
"Extended object and group tracking with elliptic random hypersurface models,"
in *Proceedings of the 13th Conference on Information Fusion (FUSION)*. IEEE, 2010, pp. 1–8.

[4] J. A. Bilmes et al.
"A gentle tutorial of the EM algorithm and its application to parameter estimation for gaussian mixture and hidden markov models,"
International Computer Science Institute, vol. 4, no. 510, p. 126, 1998.

[5] Y. Boers and J. N. Driessen
"A track before detect approach for extended objects,"
in *2006 9th International Conference on Information Fusion*. IEEE, 2006, pp. 1–7.

[6] S. Bordonaro, P. Willett, and Y. Bar-Shalom
"Consistent linear tracker with position and range rate measurements,"
in *Conference Record of the Forty Sixth Asilomar Conference on Signals, Systems and Computers (ASILOMAR)*, 2012, pp. 880–884.

[7] S. Bordonaro, P. Willett, Y. Bar-Shalom, M. Baum, and T. Luginbuhl
"Extracting speed, heading and turn-rate measurements from extended objects using the EM algorithm,"
in *Aerospace Conference, 2015 IEEE*. IEEE, 2015, pp. 1–12.

[8] A. P. Dempster, N. M. Laird, and D. B. Rubin
"Maximum likelihood from incomplete data via the EM algorithm,"
Journal of the royal statistical society. Series B (methodological), pp. 1–38, 1977.

[9] K. Gilholm, S. Godsill, S. Maskell, and D. Salmond
"Poisson models for extended target and group tracking,"
SPIE, Signal and Data Processing of Small Targets, San Diego, CA, USA, vol. 5913, p. 59130R, 2005.

[10] K. Gilholm and D. Salmond
"Spatial distribution model for tracking extended objects,"
in *Radar, Sonar and Navigation, IEE Proceedings*, vol. 152, no. 5. IET, 2005, pp. 364–371.

[11] S. Godsill, J. Li, and W. Ng
"Multiple and extended object tracking with Poisson spatial processes and variable rate filters,"
in *1st IEEE International Workshop on Computational Advances in Multi-Sensor Adaptive Processing*. IEEE, 2005, pp. 93–96.

[12] S. Granger and X. Pennec
"Multi-scale EM-ICP: A fast and robust approach for surface registration,"
in *Computer Vision—ECCV 2002*. Springer, 2002, pp. 418–432.

[13] L. Hammarstrand, L. Svensson, F. Sandblom, and J. Sorstedt
"Extended object tracking using a radar resolution model,"
IEEE Transactions on Aerospace and Electronic Systems, vol. 48, no. 3, pp. 2371–2386, 2012.

[14] W. Koch
"Bayesian approach to extended object and cluster tracking using random matrices,"
IEEE Transactions on Aerospace and Electronic Systems, vol. 44, no. 3, pp. 1042–1059, 2008.

[15] J. Lan and X. R. Li
"Tracking of extended object or target group using random matrix—part II: Irregular object,"
in *Proceedings of the 15th International Conference on Information Fusion (FUSION)*. IEEE, 2012, pp. 2185–2192.

[16] G. McLachlan and T. Krishnan
The EM algorithm and extensions.
John Wiley & Sons, 2007.

[17] D. Oakes
"Direct calculation of the information matrix via the EM,"
Journal of the Royal Statistical Society: Series B (Statistical Methodology), vol. 61, no. 2, pp. 479–482, 1999.

[18] R. Streit and T. Luginbuhl
"Probabilistic multi-hypothesis tracking,"
Technical Report 10428, Naval Undersea Warfare Center, Newport, RI February 1995 (available from DTIC), Tech. Rep., 1995.

[19] N. Ueda and R. Nakano
"Deterministic annealing EM algorithm,"
Neural Networks, vol. 11, no. 2, pp. 271–282, 1998.

[20] M. Wieneke and W. Koch
"Probabilistic tracking of multiple extended targets using random matrices,"
in *SPIE Defense, Security, and Sensing*. International Society for Optics and Photonics, 2010, pp. 769812–769812.

[21] ———
"A PMHT approach for extended objects and object groups,"
IEEE Transactions on Aerospace and Electronic Systems, vol. 48, no. 3, pp. 2349–2370, 2012.

[22] P. Willett, Y. Ruan, and R. Streit
"PMHT: Problems and some solutions,"
Aerospace and Electronic Systems, IEEE Transactions on, vol. 38, no. 3, pp. 738–754, 2002.

[23] Z. Zhang
"Iterative point matching for registration of free-form surfaces,"
Int. Journal of Computer Vision, vol. 13, no. 2, pp. 119–152, 1994.

Steven Bordonaro received his B.S. degree in Electrical Engineering from Boston University in 1991, and his M.S. degree, also in Electrical Engineering, from the University of Massachusetts. He completed a Ph.D. at the University of Connecticut in 2015. He has worked at the Naval Undersea Warfare Center in Newport, RI since 1991. His primary areas of research for the Navy and at the University of Connecticut have been signal processing, classification (machine learning) and tracking.

Peter Willett received his B.A.Sc. (Engineering Science) from the University of Toronto in 1982, and his Ph.D. degree from Princeton University in 1986. He has been a faculty member at the University of Connecticut ever since, and since 1998 has been a Professor. He was awarded IEEE Fellow status effective 2003. His primary areas of research have been statistical signal processing, detection, machine learning, data fusion and tracking. He was editor-in-chief for *IEEE Transactions on Aerospace and Electronic Systems*, and continues as VP for Publications.

Yaakov Bar-Shalom received the B.S. and M.S. degrees from the Technion, Israel Institute of Technology, in 1963 and 1967 and the Ph.D. degree from Princeton University in 1970, all in electrical engineering. From 1970 to 1976 he was with Systems Control, Inc., Palo Alto, California. Currently he is Board of Trustees Distinguished Professor in the Dept. of Electrical and Computer Engineering and Marianne E. Klewin Professor in Engineering at the University of Connecticut. He is also Director of the ESP (Estimation and Signal Processing) Lab. His current research interests are in estimation theory, target tracking and data fusion. He has published over 450 papers and book chapters in these areas and in stochastic adaptive control. He coauthored the monograph *Tracking and Data Association* (Academic Press, 1988), the graduate texts *Estimation and Tracking: Principles, Techniques and Software* (Artech House, 1993), *Estimation with Applications to Tracking and Navigation: Algorithms and Software for Information Extraction* (Wiley, 2001), the advanced graduate texts *Multitarget-Multisensor Tracking: Principles and Techniques* (YBS Publishing, 1995), *Tracking and Data Fusion* (YBS Publishing, 2011), and edited the books *Multitarget-Multisensor Tracking: Applications and Advances* (Artech House, Vol. I, 1990; Vol. II, 1992; Vol. III, 2000). He has been elected Fellow of IEEE for "contributions to the theory of stochastic systems and of multi-target tracking." He has been consulting to numerous companies and government agencies, and originated the series of Multitarget-Multisensor Tracking short courses offered via UCLA Extension, at Government Laboratories, private companies and overseas. During 1976 and 1977 he served as Associate Editor of the *IEEE Transactions on Automatic Control* and from 1978 to 1981 as Associate Editor of *Automatica*. He was Program Chairman of the 1982 American Control Conference, General Chairman of the 1985 ACC, and Co-Chairman of the 1989 IEEE International Conference on Control and Applications. During 1983–87 he served as Chairman of the Conference Activities Board of the IEEE Control Systems Society and during 1987–89 was a member of the Board of Governors of the IEEE CSS. He was a member of the Board of Directors of the International Society of Information Fusion (1999–2004) and served as General Chairman of FUSION 2000, President of ISIF in 2000 and 2002 and Vice President for Publications in 2004–13. In 1987 he received the IEEE CSS Distinguished Member Award. Since 1995 he is a Distinguished Lecturer of the IEEE AESS and has given numerous keynote addresses at major national and international conferences. He is co-recipient of the M. Barry Carlton Award for the best paper in the *IEEE Transactions on Aerospace and Electronic Systems* in 1995 and 2000 and recipient of the 1998 University of Connecticut AAUP Excellence Award for Research. In 2002 he received the J. Mignona Data Fusion Award from the DoD JDL Data Fusion Group. He is a member of the Connecticut Academy of Science and Engineering. In 2008 he was awarded the IEEE Dennis J. Picard Medal for Radar Technologies and Applications, and in 2012 the Connecticut Medal of Technology. He has been listed by academic.research.microsoft (top authors in engineering) as number 1 among the researchers in Aerospace Engineering based on the citations of his work.

Marcus Baum is an assistant research professor at the University of Connecticut. He received his Dipl.-Inform. in computer science from the the Universitaet Karlsruhe (TH), Germany, in 2007 and his a Dr.-Ing. (summa cum laude), at the Intelligent Sensor-Actuator-Systems Laboratory Karlsruhe Institute of Technology (KIT), Karlsruhe, Germany, which is a merger of Universitaet Karlsruhe and Forschungszentrum Karlsruhe. His research interests are in the field of extended object and group tracking, nonlinear estimation, and sensor data fusion. He is the associate administrative editor for the *Journal of Advances in Information Fusion (JAIF)*.

Tod Luginbuhl received a B.S. degree in electrical engineering from the University of Rochester, Rochester, NY, in 1985. He earned an M.S. and a Ph.D. in electrical engineering from the University of Connecticut, Storrs, in 1991 and 1999, respectively. He is a senior researcher in the Sensors and Sonar Systems Department at the Naval Undersea Warfare Center, where he has been employed since 1985. His research interests include data association and fusion, frequency tracking, multi-target tracking, probability density function estimation, search theory, sequential analysis, signal classification and detection, and spectrum estimation. Dr. Luginbuhl is an Associate Editor of Sequential Analysis, and a member of Eta Kappa Nu.